EVALUATION OF SOLAR AIR HEATING COLLECTION SYSTEMS FOR USE IN GRAIN DRYING USING COMPUTER SIMULATION*

G. E. Meyer, Post-Dr. Research Associate
M. A. Sabbah, Post-Dr. Research Associate
H. M. Keener, Assistant Professor
R. B. Curry, Professor
Department of Agricultural Engineering
Ohio Agricultural Research and Development Center and
The Ohio State University
Wooster, Ohio

A dynamic computer simulation model for evaluating solar air heating collection systems for grain drying was developed and tested. The heat transfer submodel of the simulator is based on a system of finite difference approximations to time-varying differential equations describing a one-dimensional heat balance of the system. Radiation losses, due to scattering and absorption of the sun's rays for flat or curved collector covers are computed using the Fresnel relations and equations by Parmelee, as a function of solar angle. Heat losses to the environment are predicted as a function of wind velocity and temperature gradients.

The computer simulation model has parameters and options, which can be controlled by the user, to study simple bare plate, suspended plate, or covered plate collectors, with flat or curved covers, with or without an integrated storage device. Simulations can be conducted for any geographical location, any collector orientation, such as tilt angle and wall-solar azimuth, a range of collector air flow rates and for any day during the calendar year. Total solar radiant flux and ambient temperature forcing data can be generated internally by the simulator or supplied as an input using actual weather records.

INTRODUCTION

Recent increases in the price of fossil fuels and difficulties in obtaining fuels meeting environmental standards has spurred a great deal of interest in the use of solar energy. For thousands of years, solar energy has been used in agriculture to dry crops and grains in the field. However, during the past 30 years, American farming has adopted early grain harvest methods and artificial drying procedures to meet market demands and to overcome unfavorable weather conditions, which deteriorates standing grain in the field. Most of the artificial drying methods require a source of supplemental heat to dry the grain, either in the form of high temperature drying or low temperature drying. The source of this heat could come partially on entirely through the collection of solar energy.

Studies concerning the use of solar energy for grain drying have been conducted over the past two years at the Ohio Agricultural Research and Development Center, Wooster, Ohio. These studies are a part of cooperative midwest studies on solar grain drying funded by the Energy Research and Development Administration (ERDA) (1). The OARDC studies include the use of computer simulation to determine the feasibility of solar energy for grain drying in Ohio. The feasibility and acceptability depends in part on the farmer being able to procure low cost, yet effective solar energy collection systems, to collect the few degrees of supplemental heat needed in a low temperature drying system.

Computer simulation offers a comprehensive and effective tool to expand the results of field tests. Solar collector simulation studies can provide reliable performance information over a wide range of environmental conditions, since the heat transfer theories and many of the solar collection processes are well known. However, the calculations required are extensive and tedious, thus requiring the use of the digital computer.

The purpose of the solar collector simulation studies was to develop a dynamic solar collector simulator that would, (1) be sensitive to time-varying inlet temperatures and solar radiation conditions, (2) simulate the basic types of collection systems currently being considered for solar grain drying, (3) provide output data suitable as input for dynamic grain drying simulation studies, and (4) to compare the simulated results with actual field results.

Description of the Model:

A dynamic simulator for evaluating the performance of solar, air heating collection systems for time-varying inlet temperatures and solar radiation was developed and tested. The model was coded in Fortran IV and compiled and executed on the IBM System/370, model 165 computer located on the Ohio State University campus at Columbus, Ohio. This system is used to support batch-processing and time-sharing systems. The time-sharing system was accessed using an ADDS Consol 980 CRT terminal and line printer located at Wooster, Ohio.

The approach taken was to model the fundamental optical and heat transfer processes, found in the basic bare plate and covered plate solar air heating

*This paper was approved for publication as Journal Article No. 155-76 of the Ohio Agricultural Research and Development Center. The research was supported by Energy Research and Development Administration.

collectors. A set of coupled non-steady state heat balance equations were written for the absorber, heat transfer fluid, and integrated storage media (e.g. the soil beneath a collector mounted flat and horizontal on the ground). In the soil media system, heat was transferred from the collector to soil during the day and then retrieved through nighttime operation of the fan moving air through the collector. Heat loss terms were aggregated into two categories; heat loss upward and heat loss downward.

Many previous and some current studies consider only steady-state collector behavior using time-averaged temperatures and radiation values. However, thermal lags and actual operating temperatures have important effects on the heat loss rate. Operating temperatures are also important in determining whether critical temperature levels are being reached, whether thermal breakdown of material may begin. For example, certain plastics being used in collector designs may begin to deteriorate at 80-90°C. It is also important to be able to simulate exhaust temperature profiles that might be used as input to dynamic grain drying simulation models (2). Thus, the ultimate effect of weather on the solar grain drying process may be readily determined.

The solar collector simulator developed at OARDC, hereafter referred to as the Ohio Solar Air Heater System (OSAHS) is composed of several submodels, which can be called upon during execution of the main program to mimic the various processes involved. Illustration 1 shows a general block diagram of the OSAHS program. The basic submodels consist of a radiation estimation submodel, a curved surface incident-radiation submodel, an optics submodel, a daylength and solar angle determination submodel, a temperature generator for calculating instantaneous outside air and soil temperature, a heat collection and storage submodel, and an integration subroutine.

Radiation Estimation Submodel:

One of the more difficult problems confronting the dynamic simulation of a solar collector is the treatment of the source of solar radiation. Unfortunately, experimental solar radiation data is generally incomplete. The OSAHS system considers direct beam, diffuse short-wave radiation, and long wave sky and absorber emitted long-wave radiation exchanges. Most solar radiation measurements are only made of total (direct beam and diffuse) radiation as energy per unit time per unit area, incident on a horizontal surface. Options are provided in the OSAHS program for handling input solar radiation values from various sources.

1. Total daily and some hourly solar radiation values are available from weather records. These values can be converted into an approximate diurnal solar radiation curve, using the equation by Cooper (3).

$$I_{DB} \cong \frac{\pi I_t}{2d} \sin\left(\frac{\pi t}{d}\right) \qquad (1)$$

ILLUSTRATION 1. Simplified Flow Diagram OSAHS Program.

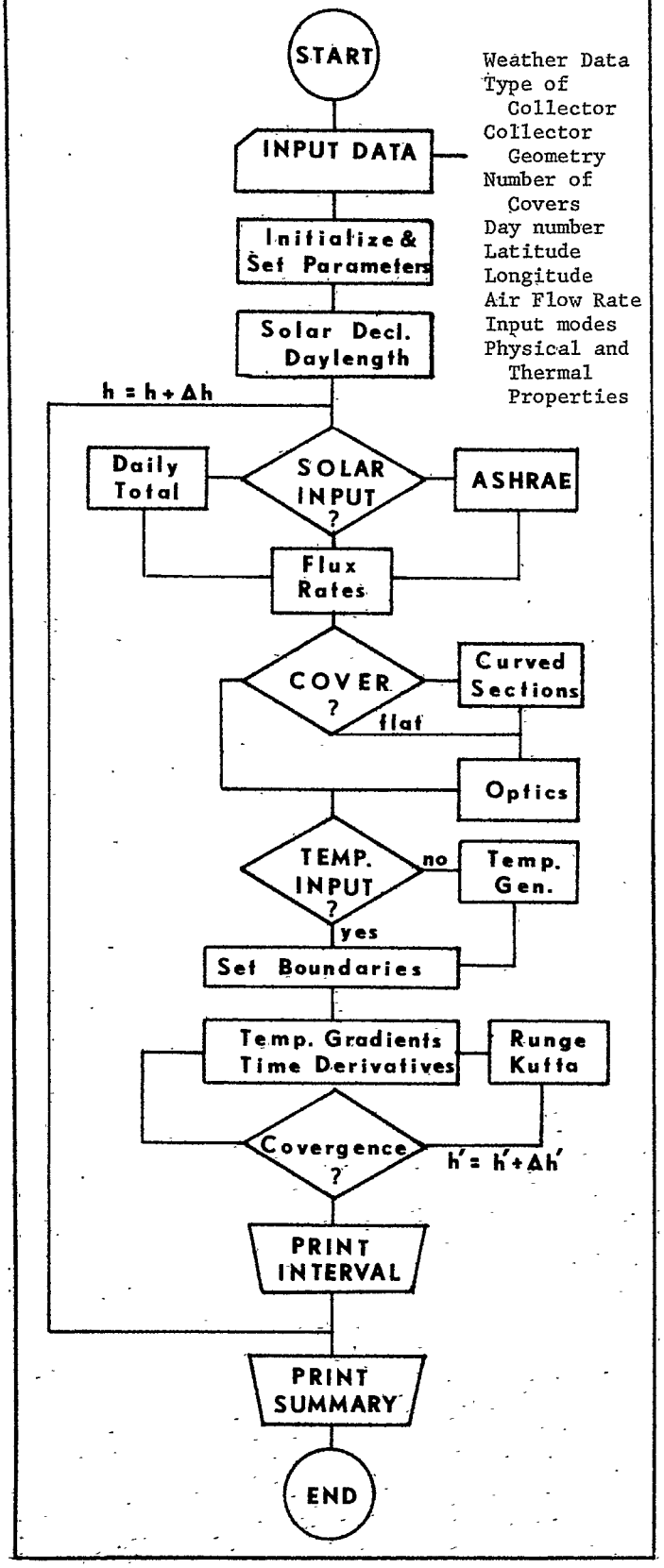

These values are then converted back to direct beam normal radiation, which are used to evaluate the effects of transparent covers for various collector orientations.

2. Estimates of direct beam normal and diffuse radiation can also be computed using the ASHRAE equations (4).

$$I_{DBN} = \frac{A}{\exp(B/\sin\beta)} \qquad (2a)$$

where $\sin\beta = \cos L \cos\delta \cos h + \sin L \sin\delta$

$$I_{DS} = C I_{DBN} F_{ss} \qquad (2b)$$

The values of A and B vary during the year, because of seasonal changes in water vapor content and dust in the atmosphere. The radiation values generated with the ASHRAE equations may not give the actual maximum values that can occur during any given month. They are intended to represent conditions on average cloudless days.

3. Instantaneous digital values of solar radiation can be read directly into OSAHS, and are converted to direct beam normal and diffuse, based on estimates of cloud conditions. Such readings were taken during some of the experimental tests conducted at OARDC.

In this study, diffuse radiation was assumed to be isotropically distributed across the sky. This assumption is probably true on days with heavy, overcast skys. During clear and lightly overcast conditions, total radiation becomes highly directional toward the location of the sun in the sky.

The value of the solar input options becomes apparent later, when considering that the calibration of the OSAHS model was conducted using radiation data available, in the form of instantaneous digital data. Once the model is calibrated, it is possible to make estimates of collector performance, even if only total daily values from the weather bureau are available. Since the ASHRAE Equations (2) are suited for general design purposes, the model can still be used when no suitable experimental radiation data are available.

Solar Angle Determination:

The OSAHS program allows the determination of the effects of various tilt angles and collector orientations. To accomplish this purpose, the equations based on the work of Benford and Bock relating the position of the sun in the sky for direct beam radiation are used (5). The angle of solar declination is computed according to Cooper (6) and is a function of the day number during the year. The length of the photoperiod or daylength is computed as a function of solar declination, latitude, and longitude. The complete set of these equations are given by Duffie and Beckman (7), ASHRAE (4), and Threlkeld (8).

Incidence Radiation on Curved Surfaces:

It became apparent at the outset, that an analysis would have to be performed to determine the transmission, absorption, and reflection effects of curved covers and curved absorber surfaces. Illustration 2 shows a cross-section of a simple covered plate collector with a curved cover. The approach, taken to determine the amount of radiation incident to the cover, was to subdivide the cover into increments. Each increment was approximated as a flat surface, at a given tilt angle as follows:

$$\sigma_i = \sigma_c + \frac{\phi_c}{2} - \Delta\phi_i \qquad (3)$$

where $\Delta\phi_i = (i - \frac{1}{2})\Delta\phi, \ (1 \le i \le n)$

and $\Delta\phi = \frac{\phi_c}{n}$

The angle ϕc is computed from base width of the collector and the radius of curvature of the cover. Then, the angle of incidence and incident radiation for the cover is computed as:

$$\cos\Theta_i = \cos\beta \cos\gamma \sin\sigma_i + \sin\beta \cos\sigma_i \qquad (4)$$

and

$$I_{ic} = \frac{1}{n}\sum_{i=1}^{n} I_{DBN} \cos\Theta_i + I_{DS} \qquad (5)$$

ILLUSTRATION 2. Cross Section of a Collector with Curved Cover.

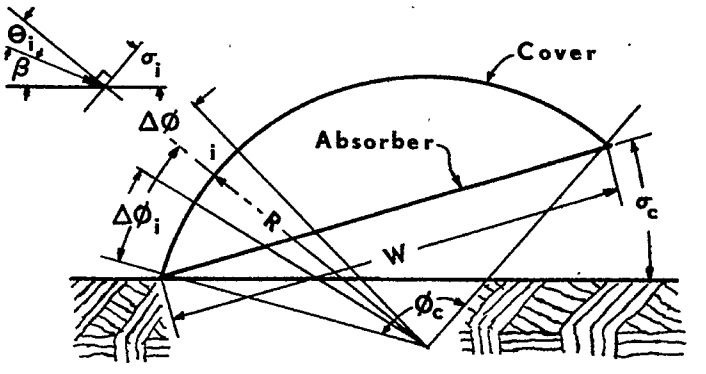

Optics Submodel:

The actual amount of radiation being absorbed, transmitted, or reflected by the cover depends on the index of refraction, extinction coefficient, and angle of incidence with the cover. Basically, these processes are functions of surface properties and are given as follows:

For reflection at the surface:

$$r_i = \frac{1}{2}\left[\frac{\sin^2(\theta_i'-\theta_i)}{\sin^2(\theta_i'+\theta_i)} + \frac{\tan^2(\theta_i'-\theta_i)}{\tan^2(\theta_i'+\theta_i)}\right] \quad (6)$$

where:

$$\theta_i' = \arcsin(N \sin\theta_i)$$

For absorption at the surface:

$$a_i = \exp(-K z_i') \quad (7)$$

where: $$z' = \frac{z}{\sqrt{1 - \frac{\sin^2\theta_i}{N^2}}}$$

The coefficient of transmission for a material of given thickness z (i.e. the distance between the two surfaces) was given by Parmelee (9) as the following:

$$\tau_i = \frac{(1-r_i)^2 a_i}{(1 - r_i^2 a_i^2)} \quad (8)$$

When considering the movement of the sun across the sky, the back of the cover may act as a reflector at low sun angles. The coefficient of reflection for the segment of the cover is $1 - \tau - \alpha$ or:

$$\rho_i = r_i + \frac{r_i(1-r_i)^2 a_i^2}{1 - r_i^2 a_i^2} \quad (9)$$

The amount or radiation transmitted through the cover and incident to the absorber, through a single curved cover is given as:

(10)

$$I_{i.a.} = I_{DBN}\frac{R\Delta\phi}{W}\left(\sum_{i=1}^{m}\tau_i\cos\theta_i + \sum_{i=m+1}^{n}\rho_i\tau_i\cos\theta_i\right) + \tau I_{DS}$$

Using the above equations, the amount of radiation incident to the absorber can be computed for either flat or curved covers. For flat covers, the radius of curvature is infinitely large and σ_i equals σ_c.

The Heat Collection and Storage Submodel:

A one-dimensional lumped parameter heat exchange submodel was developed for the collector. The submodel consisted of time-varying differential equations with pertinent temperature gradients describing the collection process. Thermal conductivities, heat capacities, density values are standard values found in ASHRAE for the materials considered. The method of solution will be described in the next section.

The following assumptions were made during the development of the model:

1. Edge effects of thermal losses from collector were assumed negligible.
2. The upward and downward heat losses were assumed to be spatially uniform and equal to energy per unit area.
3. The length of the collector was assumed to be the critical dimension with respect to temperature gradients.
4. Temperatures within the outside transparent cover were considered to be steady-state values (i.e. the cover heat capacity was considered negligible).
5. For the collection system involving heat storage in the ground beneath the collector, temperature gradients with depth and along the main axis of the collector were considered.

The following coupled equations were developed for the covered plate collector and consisted of heat balances for the absorber, air, and storage with appropriate heat loss terms.

Heat Balance for The Absorber: (11)

$$\frac{\delta T_c}{\delta t} = \frac{\alpha_{ab} I_{i.a.}}{\rho_c c_{pc} z_p} - \frac{h_v (T_c - T_a)}{\rho_c c_{pc} z_p} - \frac{\tau_w \varepsilon \sigma (T_c^4 - T_{sky}^4)}{\rho_c c_{pc} z_p} + \frac{K_p}{\rho_c c_{pc}}\frac{\delta^2 T_c}{\delta x^2} - \frac{U_{rear}(T_c - T_{ss})}{\rho_c c_{pc} z_p}$$

Heat Balance for the Air: (12)

$$\frac{\delta T_a}{\delta t} = \frac{h_v (T_c - T_a)}{\rho_a c_{pa} z_a} - \frac{\dot{m}_a}{\rho_a w z_a}\frac{\delta T_a}{\delta x} - \frac{U_{up}(T_a - T_o)}{\rho_a c_{pa} z_a}$$

Heat Balance for Storage (Soil):

Soil Surface: (13a)

$$\frac{\delta T_{ss}}{\delta t} = \frac{U_{rear}(T_c - T_{ss})}{\rho_s c_{ps} z_s} + \frac{K_s}{\rho_s c_{ps}}\left(\frac{1}{z_s}\frac{\delta T_{ss}}{\delta z} + \frac{\delta^2 T_{ss}}{\delta x^2}\right)$$

Deep Soil: (13b)

$$\frac{\delta T_s}{\delta t} = \frac{K_s}{\rho_s c_{ps}}\left(\frac{\delta^2 T_s}{\delta z^2} + \frac{\delta^2 T_s}{\delta x^2}\right)$$

The heat balance equations for the bare plate collector were written in a similar manner, except that the heat loss term in the absorber equation involves the temperature difference from the absorber to the outside air temperature and the heat loss term in the heat transfer fluid equation involves the temperature difference of the heat transfer fluid and the storage temperature. In the OSAHS program, the cover and optics submodels are disengaged, when considering the bare plate collector. These equations can be readily modified or expanded to include other storage and loss effects.

The initial temperature conditions for the absorber were approximated as steady-state temperature values calculated from the initial temperature, incident radiation, and storage temperatures. Thus, if the simulation was started at midday, the initial absorber temperature would be calculated, and the value would be found much higher than the air temperature. This approach greatly improved the stability of the numerical solutions and reduced the start-up effect.

Temperature Generator Submodel:

An option is provided in the OSAHS program for reading in instantaneous digital temperature values for the inlet air and storage (e.g. soil). A temperature generating function is also provided for calculating an empirical diurnal temperature profile from daily maximum and minimum temperatures. The function is a modification of the generator described by Soribe et. al. (10), in that, it uses four temperatures: the maximum temperatures for the past and current day and the minimum temperatures for the current and following day.

Thus, from midnight to T_{min_1} (at sunrise): (14)

$$T_a = \frac{Tmax_1+Tmin_1}{2} + \frac{Tmax_1-Tmin_1}{2}\sin\left(\frac{\pi}{2} - \frac{2\pi(h^*+2\pi)}{4\pi-d}\right)$$

From T_{min_1} to T_{max_2} (1.5 hours past solar noon):

$$T_a = \frac{Tmax_2+Tmin_1}{2} + \frac{Tmax_2-Tmin_1}{2}\sin\left(\frac{3\pi}{2} + \frac{2\pi h^*}{d}\right)$$

From T_{max_2} to midnight:

$$T_a = \frac{Tmax_2+Tmin_2}{2} + \frac{Tmax_2-Tmin_2}{2}\sin\left(\frac{\pi}{2} - \frac{2\pi h^*}{4\pi-d}\right)$$

$$h^* = h - 0.524$$

This approach eliminated all discontinuities by using just the maximum and minimum temperature for the given day, and assumes that the minimum temperature occurs just before sunrise and maximum temperature occurs 1.5 hours (lag value) past solar noon. Other lag values can be entered for different times of the year.

For calibration of model, instantaneous temperature readings were used instead of the generating function. The generating function provides an alternative for time periods when instantaneous readings are not available for design evaluations.

Integration Method:

To solve a system of time-varying differential equations, each involving different time constants required special integration procedures. Under time-varying inlet and boundary conditions, transient response characteristics of the system become very important. Wijeysundera (11) has described an analytical solution technique for arriving at the response time of multi-cover collectors with various design parameters. However, analytic solutions for several time-varying differential equations becomes more difficult to achieve, without decoupling the equations into pairs and solving as a second-order system. The technique described here involves solving the complete set of coupled equations using the fourth-order Runge-Kutta numerical method, by allowing a number of successive iterations for a set boundary value, until convergence of the solution is established. Illustration 3 shows the nodal system used for a simple covered plate collector. A five-point difference equation was used at the second node from the boundary to give a better estimate of the air temperature gradient during changing inlet temperature conditions. The gradients at the rest of the nodes were approximated as central differences.

Simulation and Results:

The solar collector model developed in the previous section, although adaptable to many kinds of solar air heaters, has been used primarily to evaluate the Soloron Collector, a prototype air supported plastic collector that was originally manufactured by the Solar Energy Products Company of Avon Lake, Ohio. Two of these collectors have been used during the past two years in experimental solar grain drying studies being conducted at OARDC (12).

The Soloron Collector is essentially a "quasi" suspended-plate collector with a high crown, curved cover and is mounted horizontally, flat on the surface at the ground. The collector dimensions are: for the width, 3.6 meters; length, 25 meters; and height, 1.2 meters. A picture of this collector is shown in Illustration 4. The collector was constructed of three layers of 10-mil vinyl UV stabilized plastic sheets; the top clear, the middle translucent, and the bottom, which is in contact with the ground, opaque. A 1/2-horsepower electric fan located at the inlet end inflates the collector and forces air predominantly between the two bottom layers of plastic. The heated air is then expelled near the inlet of the grain bin drying fan. Several collectors of this design have been used in other midwest grain drying studies.

To simulate the Soloron Collector, the collector was assumed to behave as a covered plate type collector, except that heat loss upward through the outer cover was restricted by a very low air flow rate between the upper two layers of plastic. The soil was assumed to consist of two lumps; a surface layer and a deep soil layer. The simplification of the heat transfer in the soil, was taken to facilitate computational speed. Parameter values for thermal conductivities, and optical properties for

plastic were taken from the literature and put into the model. Predicted outcomes were generally run over a simulation period of 24 hours starting at midnight (standard time). A mesh spacing of t = 0.001 hours, with the boundary values being changed every 0.03 hours was used, with the Runge-Kutta integration method. Computational times for a typical 24 hour run were not excessive. A typical 24-hour simulation, using the temperature generators and total insolation as input, took approximately 2 minutes, 20 seconds of CPU time. Handling actual instantaneous temperatures and insolation rates taken at 20 minute sample intervals took slightly longer at about 2 minutes, 50 seconds.

As previously mentioned, calibration of the Soloron model was accomplished using parameter values from the literature and instantaneous digital temperature and insolation rate data measured during experimental tests. Illustration 5 shows a calibration simulation run for data obtained on June 29, 1975, for a Soloron collector, oriented east-west, with 2.5 cm of styrofoam insulating the collector from the soil. Illustration 6 shows a run on the same day for a north-south oriented Soloron without the styrofoam insulation material. Air flow rates for both collectors were set at 49.6 m^3 min^{-1}. The actual inlet air temperatures and total instantaneous insolation rates recorded at corresponding times were read into the model prior to actual computations.

The simulation results for the predicted exhaust temperatures show reasonable agreement with the actual exhaust temperatures, for both collector configurations. Since almost three-quarters of this day was partly cloudy, the results show that the model can predict exhaust temperatures reasonably well even during intermittent cloud conditions. Slight lags existed between the actual and simulated curves. These lags appear to be due in part to the assumption that the thermal capacities of the outside covers and styrofoam were negligible, and partly to the approximation of the two-lump soil model used. It appeared that the insulated collector simulation tended to underestimate the heat capacity of the system, while the uninsulated collector simulation overestimated the heat capacity slightly.

The simulation model was then used to investigate collector performance for various air flow rates with the rest of the parameters set constant. Using October temperature and insolation data, the air flow rate was varied at several levels from 28.3 to 62.3 m^3 min^{-1}. As is demonstrated in Table 1, the lower air flow rates resulted in higher absorber temperatures and higher air temperature rises across the absorber plate. The heat collected was greater, with the higher air flow rates than with lower air flow rates. For plastic collectors, it is desirable to keep operating temperatures below 80°C to reduce thermal breakdown of the materials. Operation at high collector air flow rates for low temperature grain drying, not only results in the most efficient use of the collector, but may actually prolong the life of the plastics

The collection efficiency and heat output can also be increased by tilting the collector to an optimum tilt angle as shown in Table 2. During early October, tilting from the horizontal position to 0.87 radians resulted in an increased output of 328.7 megajoules per day or an increase of 62 percent at the given air flow rate of 49.6 m^3 min^{-1}. The maximum absorber temperatures were also increased from 82.3°C to 109.1°C. However, even when the collector is tilted, the absorber could be cooled further with higher air flow rates with conceivably greater amounts of heat output.

Most of the increase in heat output associated with tilting comes from increase in the interception of direct radiant flux. Studies using the optics submodel support this. Illustration 7 shows that by varying the tilt angle of the collector and the radius curvature of the cover, the amounts of total daily insolation incident to the absorber vary during the months of the year. For example, with the collector tilt angle of 0.87 radians, the cover intercepted the most flux during the months of February, March, September and October. When the collector is mounted at optimum tilt angle, the radius of curvature of the cover becomes more significant. For example, increasing the radius or curvature from 2.1 to 8.5 meters for the non-tilted collector during May and June decreased the reflective losses associated with the curved cover. This means that if the collector is mounted near the optimum tilt angle, a flat cover will allow more flux incident to the absorber than a curved cover.

For lower solar altitudes, which occur during the Fall drying season, the east-west orientation of the Soloron and the cover radius of curvature of 2.1 meters was found to give better performance than the north-south orientation. This has been confirmed through experimental studies (12). When the collector is oriented east-west during this period (where the back side of the cover is not directly exposed to direct rays) the back side acts as a weak reflector.

Finally, additional simulation studies were performed using insolation and temperature data obtained during soybean solar drying tests of October, 1974. A comparison of simulated and actual performance is shown in Table 3. The data for October 4, 1974 was not used because of electrical problems that occurred during field tests on that date. The simulated results presented compare favorably with the actual results, except for maximum temperature rises. The maximum temperature rises do not agree well because equation (1) has a smoothing and averaging effect on the computed flux rates. Also, it is impossible to predict the maximum temperature rise with certainty without knowing the actual solar radiation profile curve. Future research should strive to obtain such data.

Summary:

The first stages of development and verification of a dynamic solar air heater simulation model have been completed. The model was tested using data obtained from experimental studies involving

the Soloron air heater. The results of these studies indicate that the simulation process can describe quite well the exhaust temperature profiles that might occur even during cloudy conditions. More data are needed to confirm this. The simulations demonstrated that collector air flow rates have important effects on collection efficiencies and heat output. Studies on collector orientations indicated that optimum tilt angle is important in achieving the maximum heat output. The east-west orientation of the collector with a curved cover gave better performance than the north-south orientation.

Nomenclature:

I_{DB}	Incidence of direct beam radiation.
I_{DBN}	Incidence of direct beam normal to given surface.
I_{DS}	Incidence of diffuse sky radiation.
I_t	Total radiation (direct beam plus diffuse).
$I_{i.c.}$	Radiation incident to the cover.
$I_{i.a.}$	Radiation incident to the absorber.
t	Time.
d	Daylength.
β	Solar altitude.
γ	Wall-solar azimuth.
σ_i	Tilt angle for cover segment.
σ_c	Tilt angle for the collector.
R	Radius of curvature for cover.
ϕc	Arc angle of the cover.
θ	Angle of incidence.
N	Index of refraction.
r	Component reflectivity.
a	Component absorptivity.
z	Thickness of the cover.
ρ	Total reflectivity.
τ	Total transmissivity.
K	Extinction coefficient.
T_c	Absorber temperature.
T_o	Outside air temperature.
T_a	Air temperature with collector.
T_{ss}	Temperature of soil surface.
T_s	Deep soil temperature.
T_{sky}	Equivalent blackbody sky temperature.
ρ_a	Density of air.
C_{pa}	Specific heat of air.
C_{pc}	Specific heat of absorber.
ρ_c	Density of absorber.
h	Solar hour angle.
K_p	Thermal conductivity of the absorber.
K_s	Thermal conductivity of the soil.
ρ_s	Soil density.
h_v	McAdams convective heat transfer coefficient.
U_{up}	Upward heat transfer coefficient.
α	Total absorptivity of the absorber.
U_{rear}	Downward heat transfer coefficient.
A	Apparent solar irradiation at air mass = 0.
B	Atmospheric extinction coefficient.
C	Diffuse radiation factor.
F_{ss}	Angle factor between surface and sky.
L	Local latitude.
δ	Solar declination.

References:

1. Foster, G.H. and R.M. Peart. Solar Grain Drying Progress and Potential, USDA-ARS Agricultural Information Bulletin in press.

2. Bakker-Arkema, F.W., L.E. Lerew, S.F. DeBoer, and M.G. Roth. Grain Dryer Simulation. Research Report 224, The MSU and Agricultural Experiment Station, East Lansing, Michigan, 1974.

3. Cooper, P.I., Digital Simulation of Transient Solar Processes, Solar Energy 12:313-331, 1969.

4. ASHRAE Handbook of Fundamentals, Published by American Society of Heating, Refrigerating, and Air Conditioning Engineers, Inc., 1972.

5. Benford, F., and J.E. Bock, 1939. A time Analysis of Sunshine, Trans. of Am. Illum. Eng. Soc., 34:200.

6. Cooper, P.I., 1969. The Absorption of Solar Radiation in Solar Stills, Solar Energy 12:333.

7. Duffie, J.A., and W.A. Beckman, 1975. Solar Energy Thermal Processes, John Wiley & Sons, New York.

8. Threlkeld, J.L., Thermal Engironmental Engineering, Prentice-Hall, Inc., Englewood Cliffs, N.J. 1962.

9. Parmelee, G.V., Transmission of Solar Radiation through Flat Glass, ASHVE Trans. 51:317-350, 1945.

10. Soribe, F.I., Dynamic Simulation of Environment and Plant Grown in an Air-Supported Plastic Greenhouse. Unpublished Ph.D. Dissertation, The Ohio State University, 1972.

11. Wijeysundera, N.E., Response Time of Solar Collectors, Solar Energy 18:65-68, 1976.

12. Meyer, G.E., H.M. Keener, and W.L. Roller, Solar Heated Air Drying of Soybean Seed and Shelled Corn, Paper presented at 1975 Annual Meeting of American Society of Agricultural Engineers, ASAE Paper No. 75-3002, 1975.

TABLE 1. Simulated Collector Output per Day Versus Air Flow Rates[1,2].

Air Flow Rate	Max. Absorber Temperature	Max Air Temp. Rise	Avg. Air[3] Temp. Rise	Heat[3] Collected	Collection Efficiency
m^3/min (cfm)	°C (°F)	°C (°F)	°C (°F)	MJ	%
28.3 (1000)	104.4 (219.9)	33.3 (59.9)	9.2 (16.5)	437.7	30.7
39.6 (1400)	90.0 (194.0)	27.2 (48.9)	7.4 (13.3)	493.1	34.6
49.6 (1750)	82.3 (180.2)	23.1 (41.5)	6.3 (11.4)	526.4	37.0
62.3 (2200)	74.7 (166.4)	19.8 (35.7)	5.3 (9.5	557.3	39.1

[1] For Soloron Air Supported Plastic Collector, mounted in east-west orientation of principle axis, flat-horizontal ($\sigma c = 0$) and insulated from soil surface with 2.5 cm thickness, beaded styrofoam. Collection area = 90.1 m^2.
[2] Input air temperatures and total insolation based on October 7, 1975 at Wooster, Ohio; Avg. daily inlet temperature = 15.7°C, Avg. daily soil temperature = 12.2°C, Total available insolation = 1424.4 MJ. Avg. exhaust temp. (1290 m^3/min) = 29.6°C. Wind run = 100.4 Km per da.
[3] 24 hour operation.

TABLE 2. Simulated Collector Output per Day Versus Tilt Angle During October[1,2].

Tilt Angle (σc)	Max. Absorber Temperature	Max. Air Temp. Rise	Avg. Air[3] Temp. Rise	Heat[3] Collected	Collection[3] Efficiency
Radians (deg.)	°C (°F)	°C (°F)	°C (°F)	MJ	%
0. (0)	82.3 (180.2)	23.1 (41.5)	6.3 (11.4)	526.4	27
0.87 (50.0)	109.1 (228.4)	33.4 (60.1)	10.3 (18.5)	855.1	60

[1] For Soloron Air Supported Plastic Collector, mounted in east-west orientation with 2.5 cm thickness, beaded styrofoam insulation in the rear. Collection area = 90.1 m^2, Air Flow = 49.6 m^3 min^{-1}.
[2] Input air temperatures and total insolation based on October 7, 1975 at Wooster, Ohio.
[3] 24-hour operation.

TABLE 3. Comparison of Actual Versus Simulated Performance of Soloron Collector During October, 1974, Soybean Drying Tests.

Date	Actual Results[1]				Simulated Results[2]			
	Heat Output	Max. Temp. Rise	Avg. Temp. Rise	Coll. Eff.	Heat Output	Max. Temp. Rise	Avg. Temp. Rise	Coll. Eff.
	MJ/da	°C (°F)	°C (°F)	%	MJ/da	°C (°F)	°C (°F)	%
10/4/74	347.1	15.8(28.5)	3.1 (5.6)	37.3	359.6	9.4(16.9)	3.3 (5.9)	39.3
10/6/74	485.3	18.9(34.0)	4.3 (7.8)	33.6	523.3	15.1(27.1)	4.9 (8.9)	36.8
10/7/74	425.2	16.4(29.5)	3.6 (6.5)	49.3	356.6	9.1(16.4)	3.2 (5.8)	42.1
Totals	1257.6				1239.5			

[1] For Soloron Air Supported Plastic Collector, mounted in east-west orientation of principle axis, flat-horizontal ($\sigma c = 0$) and uninsulated from soil surface, Air Flow - 62.m^3 m^{-1}, collection area = 90.1m^2.
[2] Simulated using total daily insolation and temperature generator using solar radiation, wind run, and maximum and minimum temperatures reported for those dates, Air Flow - 62.3 m^3 m^{-1}, collection area = 90.1m^2.

ILLUSTRATION 3. Nodal System for Solar Air Heater Simulator.

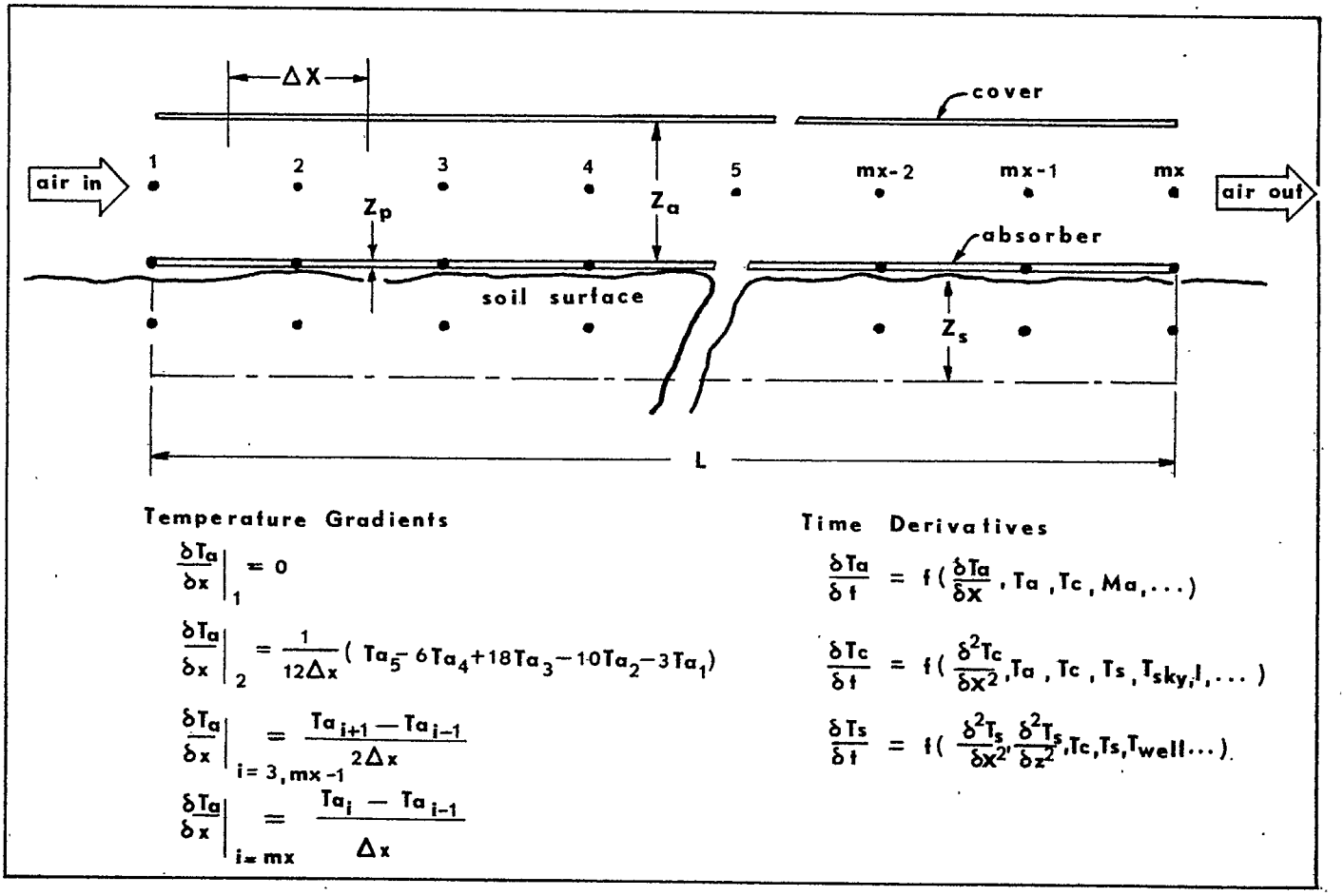

Temperature Gradients

$$\left.\frac{\delta Ta}{\delta x}\right|_1 = 0$$

$$\left.\frac{\delta Ta}{\delta x}\right|_2 = \frac{1}{12\Delta x}\left(Ta_5 - 6Ta_4 + 18Ta_3 - 10Ta_2 - 3Ta_1\right)$$

$$\left.\frac{\delta Ta}{\delta x}\right|_{i=3,mx-1} = \frac{Ta_{i+1} - Ta_{i-1}}{2\Delta x}$$

$$\left.\frac{\delta Ta}{\delta x}\right|_{i=mx} = \frac{Ta_i - Ta_{i-1}}{\Delta x}$$

Time Derivatives

$$\frac{\delta Ta}{\delta t} = f\left(\frac{\delta Ta}{\delta x}, Ta, Tc, Ma, \ldots\right)$$

$$\frac{\delta Tc}{\delta t} = f\left(\frac{\delta^2 Tc}{\delta x^2}, Ta, Tc, Ts, T_{sky,l}, \ldots\right)$$

$$\frac{\delta Ts}{\delta t} = f\left(\frac{\delta^2 T_s}{\delta x^2}, \frac{\delta^2 T_s}{\delta z^2}, Tc, Ts, T_{well} \ldots\right)$$

ILLUSTRATION 4. Soloron Plastic Solar Air Heater.

ILLUSTRATION 5. Comparison of Simulated Exhaust Temperatures Versus Actual Exhaust Temperatures.

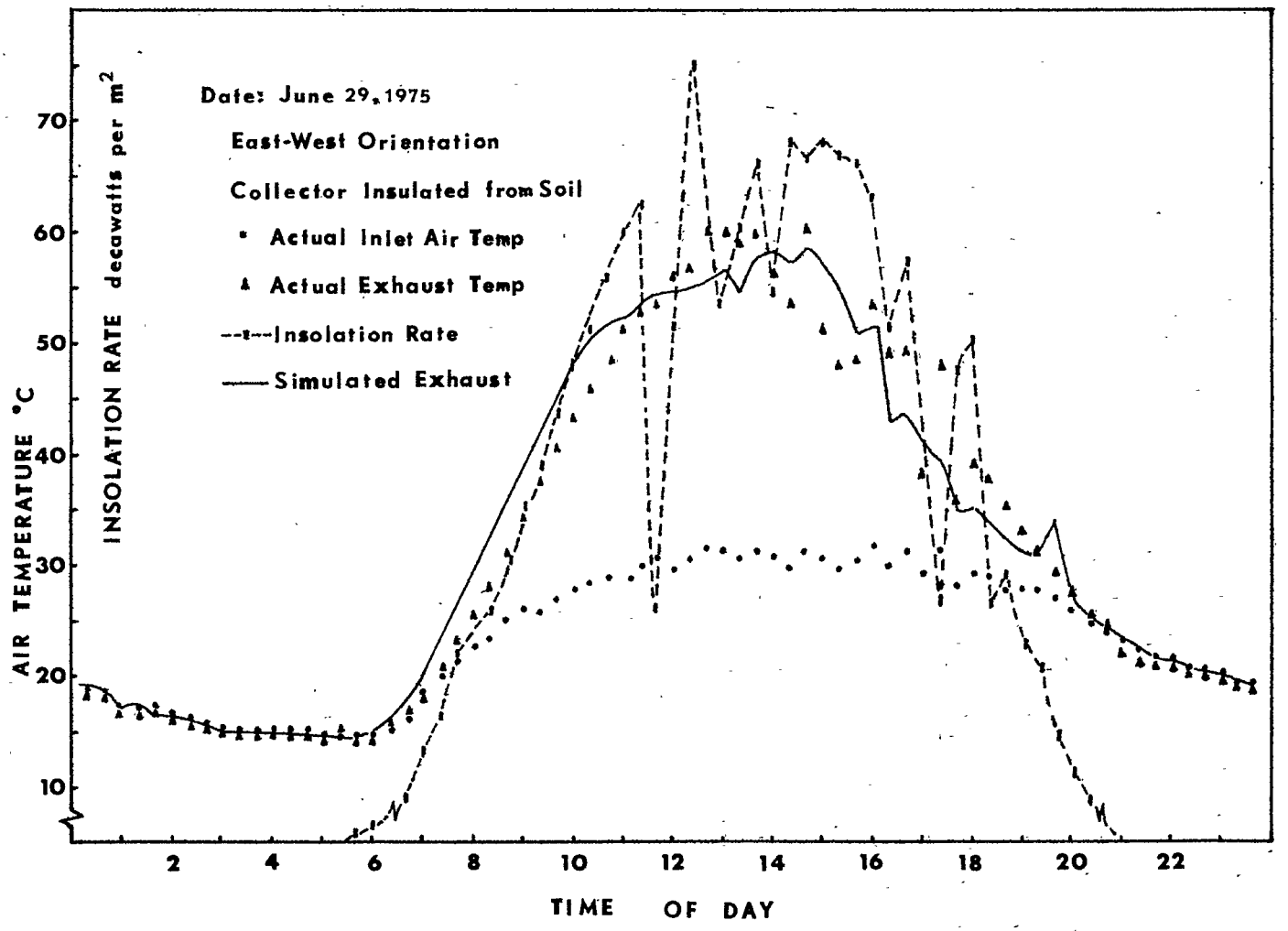

ILLUSTRATION 6. Comparison of Simulated Exhaust Temperatures Versus Actual Exhaust Temperatures.

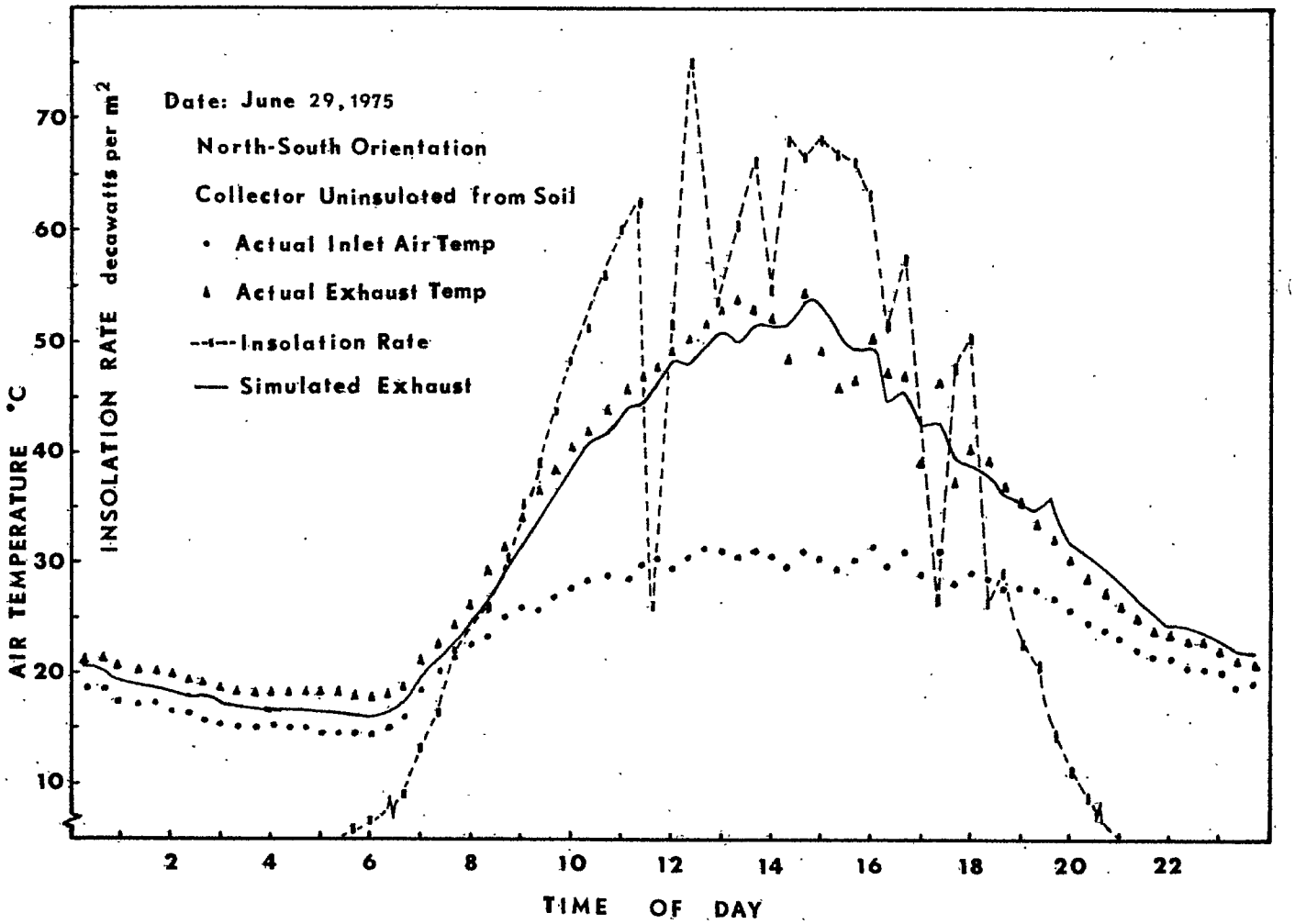

ILLUSTRATION 7. Total Daily Insolation Incident to Absorber through Curved Transparent Plastic Covers for Various Radii of Curvature and Collector Tilt Angles.